



THE UNIVERSITY *of* EDINBURGH

Edinburgh Research Explorer

Stepwise unfolding supports a subunit model for vertebrate kinetochores

Citation for published version:

Vargiu, G, Makarov, A, Allan, J, Fukagawa, T & Earnshaw, W 2017, 'Stepwise unfolding supports a subunit model for vertebrate kinetochores' Proceedings of the National Academy of Sciences, vol. 114, no. 12, pp. 3133-3138. DOI: 10.1073/pnas.1614145114

Digital Object Identifier (DOI):

[10.1073/pnas.1614145114](https://doi.org/10.1073/pnas.1614145114)

Link:

[Link to publication record in Edinburgh Research Explorer](#)

Document Version:

Peer reviewed version

Published In:

Proceedings of the National Academy of Sciences

General rights

Copyright for the publications made accessible via the Edinburgh Research Explorer is retained by the author(s) and / or other copyright owners and it is a condition of accessing these publications that users recognise and abide by the legal requirements associated with these rights.

Take down policy

The University of Edinburgh has made every reasonable effort to ensure that Edinburgh Research Explorer content complies with UK legislation. If you believe that the public display of this file breaches copyright please contact openaccess@ed.ac.uk providing details, and we will remove access to the work immediately and investigate your claim.



Stepwise unfolding supports a subunit model for vertebrate kinetochores

Giulia Vargiu¹, Alexandr A. Makarov¹, James Allan², Tatsuo Fukagawa³,
Daniel G. Booth^{1‡} and William C. Earnshaw^{1‡}

¹Wellcome Trust Centre for Cell Biology
University of Edinburgh, King's Buildings, Max Born Crescent
Edinburgh EH9 3BF, Scotland, UK

²MRC Human Genetics Unit, Institute of Genetics and Molecular
Medicine
The University of Edinburgh
Edinburgh EH4 2XU, Scotland, UK

³Laboratory of Chromosome Biology
Graduate School of Frontier Biosciences
Osaka University
Suita, Osaka 565-0871
JAPAN

‡Corresponding authors
bill.earnshaw@ed.ac.uk
daniel.booth@ed.ac.uk

1 **ABSTRACT**

2 During cell division, interactions between microtubules and
3 chromosomes are mediated by the kinetochore, a proteinaceous
4 structure located at the primary constriction of chromosomes. In
5 addition to the centromere histone CENP-A, 15 other members of the
6 Constitutive Centromere Associated Network (CCAN), participate in the
7 formation of a chromatin-associated scaffold that supports kinetochore
8 structure. We performed a targeted screen analysing unfolded
9 centrochromatin from centromere protein (CENP) depleted
10 chromosomes. Our results revealed that CENP-C and CENP-S are critical
11 for the stable folding of mitotic kinetochore chromatin. Multi-peak
12 fitting algorithms revealed the presence of an organised pattern of
13 centrochromatin packing consistent with arrangement of CENP-A
14 containing nucleosomes into up to five chromatin “subunits” – each
15 containing roughly 20-30 nucleosomes. These subunits could be either
16 layers of a boustrophedon or small loops of centromeric chromatin.
17

18 **Significant statement**

19 During cell division, microtubules apply pico-newton forces to segregate
20 duplicated chromosomes into daughter cells. The kinetochore, located
21 on the surface of the centromere chromatin, couples microtubules to
22 the chromosomes. Little is known about the folding of the centromeric
23 chromatin and how this templates the functional ultrastructure of the
24 kinetochore. To better understand this fundamental problem, we used a
25 microscopy technique that allowed the DNA associated with
26 centromeric chromatin to be unfolded and accurately measured in the
27 presence and absence of several key kinetochore components. By
28 combining this microscopy method with statistical analysis of the
29 unfolded chromatin fibres, we acquired data that allowed a subunit
30 model of the kinetochore chromatin to be proposed.

31 **\body**

32 **INTRODUCTION**

33 The centromere is the genetic locus located at the primary
34 constriction of mitotic chromosomes that directs chromosome
35 segregation. Biochemically, the centromere is defined by the presence
36 of the histone H3 variant CENP-A (1, 2) interspersed with canonical H3
37 nucleosomes carrying active chromatin marks (3, 4). This specialised
38 chromatin class has been termed ‘centrochromatin’ (5). During cell
39 division, an elaborate multi-subunit protein superstructure, the
40 kinetochore, assembles on the surface of the centrochromatin to direct
41 chromosome segregation.

42 Kinetochores contain ≥ 100 different proteins, 16 of which comprise
43 the constitutive centromere associated network (CCAN). The CCAN
44 remains associated with centromeric chromatin across the entire cell
45 cycle (6-8). The CCAN includes CENP-A, CENP-C and three multi-subunit
46 complexes: CENP-L/-N (9); CENP-H/-I/-K/-M (10); CENP-O/-P/Q-/R/-U
47 (11) and CENP-T/-W/-S/-X (12-15).

48 Although numerous immuno-electron microscopy (16-18) and
49 super-resolution microscopy (19-21) studies have mapped the locations
50 of CCAN components relative to one another, the packing of the
51 chromatin fibre in centrochromatin remains unknown. Early studies of
52 stretched chromosomes suggested a repeating “subunit” structure for
53 the kinetochore (1, 22). One subsequent hypothesis was that
54 centrochromatin is composed of “amphipathic” helices or loops, with
55 CENP-A-containing nucleosomes facing the outer kinetochore and H3
56 chromatin oriented towards the interior (5). A recent study proposed
57 that centrochromatin is folded back and forth into a sinusoidal patch or

58 boustrophedon with a multi-layered structure stabilized during mitosis
59 by CENP-C (4).

60 Here, we have dissected centrochromatin organisation by
61 progressively unfolding the chromatin at low ionic strength in lysed
62 interphase and mitotic cells. Measurement of the lengths of the
63 resulting fibres revealed that centrochromatin unfolds in a series of
64 discrete ($\sim 0.5 \mu\text{m}$) steps, consistent with a repeat substructure. CENP-C
65 and CENP-S separately contribute to the stability of the centrochromatin
66 structure during mitosis.

67

68 **RESULTS AND DISCUSSION**

69 **Step-wise unfolding of CENP-A centrochromatin**

70 To characterise the folding of centromeric chromatin, we
71 exploited the ability of low salt TEEN buffer, which lacks divalent cations
72 (see Methods) to unravel highly compact kinetochore chromatin into
73 extended fibres (23) (Fig. 1A). To identify unfolded centromeric regions
74 we generated cells expressing GFP:CENP-A from a DT40 wild type cell
75 line. Expression of exogenous GFP:CENP-A had no effect on endogenous
76 CENP-A levels (Fig. S1A). Furthermore, GFP:CENP-A was not present on
77 chromosome arms (Fig. S1B), a potential artefact associated with CENP-
78 A overexpression. GFP:CENP-A was found exclusively at the kinetochore,
79 co-localising with CENP-T, at all cell cycle stages (Fig. S1B) - even on
80 unfolded centrochromatin (Fig. S1C). This cell line was used to analyse
81 centromere unfolding in both interphase and mitotic cells (Fig. 1B).

82 We used correlative light and electron microscopy (CLEM) to
83 determine the extent of chromatin unfolding induced by TEEN
84 treatment. A line-scan analysis of correlative EM images confirmed the
85 presence of fibres with a mean diameter of 12.6 ± 2.19 nm, consistent
86 with the diameter of a single chromatin fibre (Fig. 1C). Thus, TEEN
87 treatment can unfold chromatin to the level of single fibres.

88 Collective analysis of >1300 individual centrochromatin fibres
89 revealed that interphase prekinetochores unfolded to a significantly
90 greater extent than mitotic kinetochores (unfolded length of CENP-A
91 domain - 1.664 ± 0.049 μ m versus 0.936 ± 0.025 μ m [median \pm SEM]
92 respectively, Fig. 1D). The increased stability presumably allows mitotic
93 kinetochores to resist forces applied by spindle microtubules during
94 chromosome movements.

95 To confirm that only single centromeres were analysed we
96 measured GFP:CENP-A fluorescence levels as a function of chromatin
97 fibre length (Fig. 1E). Total GFP:CENP-A amounts remained constant
98 across a range of fibre lengths up to 2.5 μm (mean = $32240.46 \pm$
99 3872.53). This strongly suggests that each unfolded CENP-A “subunit”
100 analysed consists of a single unfolded centromere.

101 To determine whether centromeres unfold at random or in
102 discrete steps, we analysed the distribution of unfolded fiber lengths
103 using frequency histograms and multi-peak fitting algorithms to reveal
104 periodicities in the data. Our comprehensive datasets (>650
105 measurements per sample) allowed us to generate high-resolution
106 histograms (100 x 0.1 μm bins). This revealed the apparent presence of
107 sub-populations of unfolded fibres, an observation masked with coarser
108 bin widths (Fig. S2A). We then defined the periodicities observed (Fig.
109 S2B), using the multi-peak fitting software Igor Pro 6.2 (WaveMetrics,
110 Inc.) (see Methods). Five distinct peaks were recognised in interphase
111 unfolded centrochromatin (Fig. 2A) and only three peaks in its mitotic
112 counterpart (Fig. 2B). Each peak represented a node of accumulation of
113 subpopulations of fibres, each corresponding to a potential “subunit” of
114 centrochromatin released from the kinetochore.

115 To estimate the amount of DNA present in each unfolding
116 “subunit” we determined the density of nucleosome packing in mitotic
117 chromatin fibres unfolded under these conditions by analysing TEM of
118 chromosome spreads prepared in TEEN buffer. The average center-to-
119 center distance between adjacent nucleosomes was 20.43 ± 0.68 nm
120 (Fig. S3A). The comparable distance from chicken erythrocyte interphase
121 chromatin in low salt buffer was 38.71 ± 1.6 nm (Fig. S3B). These

122 numbers could not be measured specifically at centromeres, and thus
123 provide only baseline values for estimating the chromatin packing.

124 Having measured peak locations and an approximate
125 internucleosome distance we could estimate the amount of DNA
126 present within the kinetochore. The distance between the fibre origin,
127 the first peak, and pairs of adjacent peaks (steps) were interpreted as
128 measures of chromatin length per unfolding “subunit”. Interphase fibres
129 unfolded in 5 steps with a mean step size of $0.69 \pm 0.24 \mu\text{m}$ (Fig. 3A).
130 Assuming 200 bp per average nucleosome, this corresponds to 17.8 Kbp
131 of DNA (Fig. S3C). In mitosis, we identified three more variable steps
132 ($0.83 \pm 0.33 \mu\text{m}$) corresponding to roughly 24.4 Kbp of chromatin (Figs.
133 3B, S3C). These estimates of DNA content assume that the
134 centrochromatin unfolds completely and are therefore almost certainly
135 underestimates.

136 If we exclude the first step, subsequent steps of unfolding of
137 interphase chromatin are remarkably reproducible, with a step size of
138 $0.58 \pm 0.1 \mu\text{m}$, corresponding to roughly 15 nucleosomes (Fig. 3A).
139 Interestingly, the first step is almost exactly twice this. A similar
140 consideration of the mitotic unfolding is more speculative, given the
141 apparent variable spacing and small number of steps. However, the
142 minimum observed step ($0.45 \mu\text{m} - \sim 22$ nucleosomes), is close to the
143 average step size observed for interphase chromatin, and again, almost
144 exactly half the length of the first step.

145 Remarkably, a recent paper looking at human centromeres
146 calculated that 1 in 25 centromeric nucleosomes contains CENP-A (24).
147 Although the corresponding measurements have not been made for
148 DT40 cells, the correlation with the average “subunit” size measured

149 here is striking. It is therefore possible that each centrochromatin
150 “subunit” is organised around a single CENP-A nucleosome in DT40 cells.

151 It is tempting to speculate that unfolding of centrochromatin in
152 low ionic strength buffer begins for interphase chromatin with two
153 “subunits”, followed by four individual steps, and in mitotic chromatin
154 with two steps of one single “subunit”. The differences in total length
155 suggest either that the CENP-A chromatin domain is smaller in mitosis
156 compared to interphase or (more likely) that the mitotic chromatin is
157 more constrained and unfolds only partly.

158 What are the “subunits” likely to be? Given that they correspond
159 to roughly 20-30 nucleosomes, we suggest that it is unlikely that they
160 would correspond to gyres of a chromatin helix (Fig. 4A). The solenoid as
161 described by Finch and Klug was proposed to have from 4 to 10 subunits
162 per turn (25), and increasing this 2 or 3-fold would give rise to chromatin
163 fibres much wider than typically seen. They could, however, correspond
164 to folded loops (Fig. 4B) or to successive layers of a boustrophedon (a
165 stack of planar sinusoidal patches) (Fig. 4C) (4). Interestingly, the typical
166 width of a kinetochore plate measured by electron microscopy in DT40
167 cells is 227 nm (26). This would easily accommodate layers containing 25
168 nucleosomes inter-linked by other components of the CCAN.

169

170 **The role of CCAN proteins in the maintenance of kinetochore** 171 **chromatin folding**

172 To further dissect the role of individual CCAN components in
173 stabilising “subunit” interactions in centrochromatin, we analysed fibre
174 unfolding following the depletion of specific CENPs. This analysis used
175 conditional knockouts (designated GENENAME^{ON/OFF}) for CENP-C; CENP-

176 H, CENP-I (from the CENP-H/-I/-K/-M complex); CENP-N (from the CENP-
177 L/-N complex); CENP-T/-W (from the CENP-T/-W/-S/-X complex); Ndc80
178 (from the Ndc80 complex); and absolute knockouts (designated
179 GENENAME^{KO}) for the non-essential proteins CENP-S and CENP-O (from
180 the CENP-O/-P/-Q/-R/-U complex). Generation of these knockout cell
181 lines was previously described (4, 7, 14, 26-32). We confirmed that the
182 growth properties of each cell line remained as previously described for
183 the original knockouts (Figs. S4B, S5B).

184 Each mutant cell line was engineered to stably express GFP:CENP-
185 A. GFP:CENP-A colocalized with CENP-T at centromeres both in the
186 presence or absence of doxycycline (Fig. S4A). CENP-T localization was
187 decreased following CENP-H and CENP-I depletion and abolished in
188 CENP-N, CENP-T and CENP-W mutants (Fig. S5A). Immunoblotting
189 analysis showed some variability in the expression levels of the total
190 CENP-A across the cell lines (Figs. S4C, S5C, S6).

191 To examine the role of individual proteins in the stability of
192 mitotic kinetochore chromatin, cells were depleted of target proteins
193 (+dox or +aux) and synchronized in mitosis, before processing for fibre
194 analysis. A striking difference in the median unfolded length was seen
195 between mitotic centrochromatin fibres from wild type (0.936 ± 0.025
196 μm) and both CENP-C^{OFF} ($2.207 \pm 0.135 \mu\text{m}$) and CENP-S^{KO} (1.66 ± 0.143
197 μm) cells (Fig. 5A). Strikingly, CENP-C depletion resulted in an even
198 greater extension of the mitotic centromere than was seen with wild
199 type interphase fibres ($1.664 \mu\text{m} \pm 0.049$; $p < 0.0001$) (Fig. 5A).

200 Small, albeit statistically significant changes were also observed
201 following the depletion of CENP-H, CENP-T, CENP-I and CENP-N (Fig. 5A).
202 These effects are small, and in an earlier, less extensive, study depletion

203 of CENP-H appeared not to affect the stability of the mitotic kinetochore
204 (4). No destabilization was observed for mitotic centrochromatin fibres
205 from CENP-O^{KO}, Ndc80^{OFF} or CENP-W^{OFF} cells.

206 Analysis of the unfolding step sizes for mitotic centrochromatin,
207 revealed the existence of two classes of mutants (Figs. 3, S7, S8). The
208 first, composed of CENP-H^{OFF}, CENP-I^{OFF}, Ndc80^{OFF}, CENP-O^{KO}, CENP-N^{OFF},
209 CENP-W^{OFF} and CENP-T^{AID} cells (Figs. 3, S7, S8), showed a mean unfolding
210 step of $0.49 \pm 0.05 \mu\text{m}$ (compared to $0.45 \mu\text{m}$ for wild type mitotic
211 centrochromatin), which was preceded by a mean step of 0.76 ± 0.04
212 μm ($0.81 \mu\text{m}$ in wild type). No third step was seen in these samples,
213 possibly due to the decreased sample size, as that step corresponded to
214 only 3% of unfolded kinetochore fibres from mitotic wild type cells.
215 These data reveal that mitotic centrochromatin from CENP-H^{OFF}, CENP-
216 I^{OFF}, Ndc80^{OFF}, CENP-O^{KO}, CENP-N^{OFF}, CENP-W^{OFF} and CENP-T^{AID} cells
217 apparently unfolds like wild type centrochromatin. Therefore, these
218 kinetochore components play at most a minor role in stabilising the
219 mitotic kinetochore chromatin packing as detected by this assay.

220 In contrast, the unfolding pattern exhibited by centrochromatin
221 from CENP-C^{OFF} and CENP-S^{KO} cells was very different from that seen
222 with either wild type or the other mutants (Figs. 3, S7). Unfolding
223 involved four steps instead of the three seen in wild type, and in
224 contrast to the other examples, the unfolding proceeded in relatively
225 equal steps (i.e. not two “subunits” followed by one). Furthermore, each
226 step was roughly twice the length of the minimum step seen for wild
227 type. Thus, mitotic centrochromatin from CENP-C^{OFF} and CENP-S^{KO} cells
228 unfolded with a mean step size of $1.172 \pm 0.12 \mu\text{m}$ and $1.110 \pm 0.08 \mu\text{m}$,
229 respectively (Fig. 3C, D). This is consistent with a model where CENP-C

230 and CENP-S are required to link adjacent centrochromatin “subunits”
231 (e.g. loops or layers of a boustrophedon) together.

232 In addition to the different step size, unfolded centrochromatin
233 fibres from CENP-S^{KO} and CENP-C^{OFF} cells average 1.8 - 2.4 – times longer
234 than the corresponding fibres from wild type (Fig. 5A). Thus, in addition
235 to causing a different pattern of unfolding, the loss of CENP-C and CENP-
236 S also results in a greater overall extent of kinetochore unfolding. This
237 reinforces the conclusion that the organisation of the kinetochore
238 chromatin in these mutant cells is significantly different from that in wild
239 type.

240 Importantly, interphase centrochromatin from CENP-C^{OFF} and
241 CENP-S^{KO} cells behaves very differently (Fig. 5B). CENP-C^{OFF} interphase
242 centrochromatin unfolds to the same extent as wild type, but CENP-S^{KO}
243 interphase centrochromatin unfolds to a significantly greater extent.
244 This strongly suggests that even though both proteins are required for
245 the stabilisation of centrochromatin, they may do so via distinct
246 mechanisms.

247 Our data support previous conclusions that the inner kinetochore
248 protein CENP-C (17, 20), forms a nexus for multiple interactions that
249 stabilise the mitotic kinetochore, amongst other things, determining the
250 diameter of the outer kinetochore plate (33). Indeed, CENP-C is required
251 to efficiently recruit both inner and outer kinetochore components
252 during kinetochore assembly (34-37).

253 The destabilization of mitotic kinetochores in CENP-S^{KO} cells was
254 surprising. CENP-S is part of the hetero-tetrameric CENP-T/-W/-S/-X
255 complex (12). However, loss of CENP-W had no effect and CENP-T only a
256 minor effect on centrochromatin stability in our assay. Detectable

257 (though reduced) levels of CENP-T are retained at kinetochores of CENP-
258 S^{KO} cells, and chromosomes appear to contain both CENP-T/-W and
259 CENP-T/-W/-S/-X complexes (37) (Fig. S4A). Similarly to CENP-C, an
260 electron microscopy study reported that CENP-S depletion could affect
261 kinetochore plate size (26).

262 Consistent with these effects on kinetochore plate size,
263 quantitation of immunoblots revealed that the total CENP-A levels were
264 lowest in CENP-C^{OFF} and CENP-S^{KO} cell lines (Fig. S6). However human
265 cells normally contain excess CENP-A molecules (24), and chicken cells
266 survive up to 4 days following CENP-A depletion, by which time CENP-A
267 molecules have been diluted 12-fold (38). The lower level of CENP-A is
268 unlikely to explain the centrochromatin destabilization in those mutants
269 since there is very little difference in total CENP-A levels between CENP-
270 C^{OFF} and CENP-I^{OFF} cells even though the centrochromatin is destabilized
271 in one and normal in the other.

272 Possible roles of CENP-S at the kinetochore are complicated by the
273 fact that this protein also functions in DNA repair. CENP-S/MHF1 has a
274 role in the resolution of DNA interstrand crosslinks and sister chromatid
275 exchanges (SCEs) by the Fanconi Anemia complex. CENP-S is required for
276 chromatin targeting and stability of the FANCM subcomplex, of which it
277 is a member together with CENP-X/MHF2 (39, 40). In DT40 cells, SCEs
278 increased 3-4 fold when CENP-S/MHF1 was depleted (39, 40). Thus,
279 CENP-S involvement in centrochromatin stability may reflect a more
280 general role in chromatin higher-order structure across the cell cycle.

281 Our results suggest that CENP-H/-I/-K/-M and Ndc80 complexes
282 act within individual centrochromatin subunits, or between subunits and
283 non-chromatin components of the kinetochore. In contrast, CENP-C has

284 a web of interactions with other CCAN members, including CENP-A and
285 CENP-H/-I/-K/-M (35, 36, 41) as well as outer kinetochore components
286 (10, 42). CENP-T/W/S/X also interacts both with CENP-H/-I/-K/-M (10)
287 and the Ndc80 complex (13, 43). We considered whether interactions
288 between the inner and outer kinetochore might stabilise mitotic
289 centrochromatin, but this is unlikely, as kinetochores lacking Ndc80 have
290 a “subunit” organisation and mitotic stability similar to wild type (Figs.
291 3H, 5A).

292 The dependencies on centrochromatin stability observed here do
293 not appear to correspond to the recent description of “core” and
294 “expandable” kinetochore modules described recently in *Xenopus*
295 extracts (44). There, CENP-A, CENP-H/-I/-K/-M, CENP-T/W/S/X and
296 Ndc80 were all found to part of the “core” kinetochore that was
297 unaffected by the loss of microtubules, whereas CENP-C was involved in
298 the expansion that occurred when microtubules were absent. The
299 authors suggested that this expansion did not involve the
300 centrochromatin, but rather corresponded to a polymerization of
301 protein complexes, in which the multifunctional CENP-C played a key
302 role. This is consistent with our observation that both a “core”
303 component (CENP-S) and an “expandable” component (CENP-C) are
304 involved in mitotic centrochromatin stability.

305 The role of CENP-O/-P/-Q/-R/-U in kinetochore organisation
306 remains enigmatic. Studies in *S. cerevisiae* report a role for the COMA
307 complex (CENP-O/-P/-Q/-R/-U complex homolog) in the looping of
308 centromere chromatin (45). However our results plus other recent
309 studies have failed to identify a function for this complex in vertebrate
310 kinetochores (37, 41).

311 Given the measurements of internucleosome distance in bulk
312 chromatin of mitotic chromosomes and interphase nuclei unfolded in
313 low salt buffer (23), we estimated the amount of DNA present at
314 kinetochores in the different cell lines. According to the lengths
315 measured for CENP-A fibres, these values ranged of 12 to 45 Kbp. The
316 smaller number likely corresponds to fibres that were not completely
317 unfolded, whereas the larger number (from unfolded CENP-C^{OFF} and
318 CENP-S^{KO} chromosomes) was remarkably close to the estimated 50-60
319 kb of DNA in chicken kinetochores determined by quantitative
320 fluorescence microscopy (46), and the ~ 40 kb of DNA occupied by
321 CENP-A in chicken non-repetitive centromeres and neocentromeres,
322 determined by CHIP (47).

323 In the future, it will be important to devise super-resolution
324 imaging strategies in which a centrochromatin fibre can be traced in
325 intact mitotic chromosomes. A recent study revealed that kinetochores
326 form large crescents during early prometaphase when they are
327 “searching” for microtubules, and become more compact structures
328 once the attachments have matured (48). This raises an extremely
329 interesting fundamental question of whether the underlying chromatin
330 reorganization also changes at this time.

331

332 **MATERIALS AND METHODS**

333 Detailed electron microscopy procedures are described in the SI
334 Materials and Methods.

335

336 **Fibre length preparation and length measurements**

337 Chromatin fibres were prepared using TEEN buffer (10 mM
338 Triethanolamine:HCl pH 8.0, 10 mM NaCl, 5 mM EDTA) using an
339 optimised version of a previously described method (49). GFP:CENP-A
340 unfolded centrochromatin was imaged using a CCD camera (CoolSnap
341 HQ, Photometrix) on a wide-field microscope (DeltaVision Spectris;
342 Applied Precision) with a NA 1.4 Plan Apochromat 100X lens controlled
343 by DeltaVision SoftWorx (Applied Precision). ImageJ (National Institute
344 of Health, Bethesda, MD) segmented line tool was used to measure
345 centromere chromatin fibre length.

346

347 **Multi-peak analysis**

348 Fibre unfolding data was imported in Igor Pro 6.2 (WaveMetrics, Inc.).
349 Data sets were allotted into the appropriate number of histogram bins.
350 The multi-peak fitting 2.0 package was used for peak identification using
351 “Auto-Locate Peaks Now”. This automatic peak finding algorithm
352 searches for and identifies subpopulations by finding maxima in the
353 smoothed second derivative of the data. To achieve this, the algorithm
354 estimates both the noise level and optimum smoothing factor of the
355 data. All adjustable parameters were kept within the same range across
356 all samples: noise level 0.00005-0.06; smooth fraction 0.05-2.5; minimal
357 fraction 0.035-0.5. After an initial estimation of the peaks the fitting
358 algorithm was run and results were summarised in a table containing

359 information about peak location, area, type, amplitude and residuals.
360 Residuals, or fitting deviations, represent the difference between the
361 observed values with the predicted sample mean and the best fit curve.
362 A positive value of residuals suggest that the measured value is placed
363 above the best fitting curve whilst a negative one is referred to a value
364 located underneath it. If the best fit curve passes through the value
365 measured then the residuals equal zero. According to Igor Pro guidelines
366 good fitting is achieved when deviation of the residuals is less then 0.1.
367
368

369 **ACKNOWLEDGMENTS**

370 This work was funded by The Wellcome Trust, of which WCE is a
371 Principal Research Fellow [grant number 107022]. The Wellcome Trust
372 Centre for Cell Biology is supported by core grant numbers 077707 and
373 092076 and Wellcome Trust Multi User Equipment Grant
374 (WT104915MA). This work was supported by JSPS KAKENHI Grant
375 Number JP25221106 and JP15H05972 to TF. GV was supported by a
376 studentship from the Darwin Trust of Edinburgh.

377

378 **AUTHOR CONTRIBUTIONS**

379 GV, Acquisition of the data, Analysis and interpretation of the data,
380 Drafting and revising the article critically for important intellectual
381 content; AAM, Acquisition of the data; JA, Acquisition of the data; TF,
382 Contributed with essential reagents, Revising the article critically for
383 important intellectual content, Final approval of the version to be
384 published; DGB, Acquisition of the data, Analysis and interpretation of
385 the data, Design, Revising the article critically for important intellectual
386 content, Final approval of the version to be published; WCE, Conception
387 and design, Analysis and interpretation of the data, Revising the article
388 critically for important intellectual content, Final approval of the version
389 to be published.

390

391 **CONFLICT OF INTEREST**

392 The authors declare that no competing interests exist.

393

394
395
396
397
398
399
400
401
402
403
404
405
406
407
408
409
410
411
412
413
414
415
416
417
418
419
420
421
422
423
424
425
426
427
428
429
430
431
432
433
434
435
436
437
438
439
440

References

1. Earnshaw WC & Rothfield N (1985) Identification of a Family of Human Centromere Proteins Using Autoimmune Sera from Patients with Scleroderma. *Chromosoma* 91(3-4):313-321.
2. Palmer DK, O'Day K, Trong HL, Charbonneau H, & Margolis RL (1991) Purification of the centromere-specific protein CENP-A and demonstration that it is a distinctive histone. *Proceedings of the National Academy of Sciences of the United States of America* 88(9):3734-3738.
3. Blower MD, Sullivan BA, & Karpen GH (2002) Conserved organization of centromeric chromatin in flies and humans. *Dev Cell* 2(3):319-330.
4. Ribeiro SA, Vagnarelli P, Dong Y, Hori T, McEwen BF, *et al.* (2010) A super-resolution map of the vertebrate kinetochore. *Proceedings of the National Academy of Sciences of the United States of America* 107(23):10484-10489.
5. Sullivan BA & Karpen GH (2004) Centromeric chromatin exhibits a histone modification pattern that is distinct from both euchromatin and heterochromatin. *Nature structural & molecular biology* 11(11):1076-1083.
6. Foltz DR, Jansen LE, Black BE, Bailey AO, Yates JR, 3rd, *et al.* (2006) The human CENP-A centromeric nucleosome-associated complex. *Nature cell biology* 8(5):458-469.
7. Okada M, Cheeseman IM, Hori T, Okawa K, McLeod IX, *et al.* (2006) The CENP-H-I complex is required for the efficient incorporation of newly synthesized CENP-A into centromeres. *Nature cell biology* 8(5):446-457.
8. Izuta H, Ikeno M, Suzuki N, Tomonaga T, Nozaki N, *et al.* (2006) Comprehensive analysis of the ICEN (Interphase Centromere Complex) components enriched in the CENP-A chromatin of human cells. *Genes to cells : devoted to molecular & cellular mechanisms* 11(6):673-684.
9. Hinshaw SM & Harrison SC (2013) An Iml3-Chl4 heterodimer links the core centromere to factors required for accurate chromosome segregation. *Cell reports* 5(1):29-36.
10. Basilico F, Maffini S, Weir JR, Prumbaum D, Rojas AM, *et al.* (2014) The pseudo GTPase CENP-M drives human kinetochore assembly. *eLife* 3:e02978.
11. Eskat A, Deng W, Hofmeister A, Rudolphi S, Emmerth S, *et al.* (2012) Step-wise assembly, maturation and dynamic behavior of the human CENP-P/O/R/Q/U kinetochore sub-complex. *PloS one* 7(9):e44717.
12. Nishino T, Takeuchi K, Gascoigne KE, Suzuki A, Hori T, *et al.* (2012) CENP-T-W-S-X forms a unique centromeric chromatin structure with a histone-like fold. *Cell* 148(3):487-501.
13. Schleiffer A, Maier M, Litos G, Lampert F, Hornung P, *et al.* (2012) CENP-T proteins are conserved centromere receptors of the Ndc80 complex. *Nature cell biology* 14(6):604-613.
14. Hori T, Amano M, Suzuki A, Backer CB, Welburn JP, *et al.* (2008) CCAN makes multiple contacts with centromeric DNA to provide distinct pathways to the outer kinetochore. *Cell* 135(6):1039-1052.

- 441 15. Dornblut C, Quinn N, Monajambashi S, Prendergast L, van Vuuren C, *et al.*
442 (2014) A CENP-S/X complex assembles at the centromere in S and G2
443 phases of the human cell cycle. *Open biology* 4:130229.
- 444 16. Cooke CA, Bernat RL, & Earnshaw WC (1990) CENP-B: a major human
445 centromere protein located beneath the kinetochore. *The Journal of cell*
446 *biology* 110(5):1475-1488.
- 447 17. Saitoh H, Tomkiel J, Cooke CA, Ratrie H, 3rd, Maurer M, *et al.* (1992)
448 CENP-C, an autoantigen in scleroderma, is a component of the human
449 inner kinetochore plate. *Cell* 70(1):115-125.
- 450 18. Suzuki A, Hori T, Nishino T, Usukura J, Miyagi A, *et al.* (2011) Spindle
451 microtubules generate tension-dependent changes in the distribution of
452 inner kinetochore proteins. *The Journal of cell biology* 193(1):125-140.
- 453 19. Joglekar AP, Bloom K, & Salmon ED (2009) In vivo protein architecture of
454 the eukaryotic kinetochore with nanometer scale accuracy. *Curr Biol*
455 19(8):694-699.
- 456 20. Wan X, O'Quinn RP, Pierce HL, Joglekar AP, Gall WE, *et al.* (2009) Protein
457 architecture of the human kinetochore microtubule attachment site. *Cell*
458 137(4):672-684.
- 459 21. Suzuki A, Badger BL, Wan X, DeLuca JG, & Salmon ED (2014) The
460 architecture of CCAN proteins creates a structural integrity to resist
461 spindle forces and achieve proper Intrakinetochore stretch. *Dev Cell*
462 30(6):717-730.
- 463 22. Zinkowski RP, Meyne J, & Brinkley BR (1991) The centromere-
464 kinetochore complex: a repeat subunit model. *The Journal of cell biology*
465 113(5):1091-1110.
- 466 23. Earnshaw WC & Laemmli UK (1983) Architecture of metaphase
467 chromosomes and chromosome scaffolds. *The Journal of cell biology*
468 96(1):84-93.
- 469 24. Bodor DL, Mata JF, Sergeev M, David AF, Salimian KJ, *et al.* (2014) The
470 quantitative architecture of centromeric chromatin. *eLife* 3:e02137.
- 471 25. Finch JT & Klug A (1976) Solenoidal model for superstructure in
472 chromatin. *Proceedings of the National Academy of Sciences of the United*
473 *States of America* 73(6):1897-1901.
- 474 26. Amano M, Suzuki A, Hori T, Backer C, Okawa K, *et al.* (2009) The CENP-S
475 complex is essential for the stable assembly of outer kinetochore
476 structure. *The Journal of cell biology* 186(2):173-182.
- 477 27. Fukagawa T, Mikami Y, Nishihashi A, Regnier V, Haraguchi T, *et al.* (2001)
478 CENP-H, a constitutive centromere component, is required for
479 centromere targeting of CENP-C in vertebrate cells. *The EMBO journal*
480 20(16):4603-4617.
- 481 28. Nishihashi A, Haraguchi T, Hiraoka Y, Ikemura T, Regnier V, *et al.* (2002)
482 CENP-I is essential for centromere function in vertebrate cells. *Dev Cell*
483 2(4):463-476.
- 484 29. Hori T, Haraguchi T, Hiraoka Y, Kimura H, & Fukagawa T (2003) Dynamic
485 behavior of Nuf2-Hec1 complex that localizes to the centrosome and
486 centromere and is essential for mitotic progression in vertebrate cells.
487 *Journal of cell science* 116(Pt 16):3347-3362.

- 488 30. Kwon MS, Hori T, Okada M, & Fukagawa T (2007) CENP-C is involved in
489 chromosome segregation, mitotic checkpoint function, and kinetochore
490 assembly. *Molecular biology of the cell* 18(6):2155-2168.
- 491 31. Hori T, Okada M, Maenaka K, & Fukagawa T (2008) CENP-O class proteins
492 form a stable complex and are required for proper kinetochore function.
493 *Molecular biology of the cell* 19(3):843-854.
- 494 32. Wood L, Booth DG, Vargiu G, Ohta S, deLima Alves F, *et al.* (2016)
495 Auxin/AID versus conventional knockouts: distinguishing the roles of
496 CENP-T/W in mitotic kinetochore assembly and stability. *Open biology*
497 6(1):150230.
- 498 33. Tomkiel J, Cooke CA, Saitoh H, Bernat RL, & Earnshaw WC (1994) CENP-C
499 is required for maintaining proper kinetochore size and for a timely
500 transition to anaphase. *The Journal of cell biology* 125(3):531-545.
- 501 34. Hori T, Shang WH, Takeuchi K, & Fukagawa T (2013) The CCAN recruits
502 CENP-A to the centromere and forms the structural core for kinetochore
503 assembly. *The Journal of cell biology* 200(1):45-60.
- 504 35. Nagpal H, Hori T, Furukawa A, Sugase K, Osakabe A, *et al.* (2015) Dynamic
505 changes in CCAN organization through CENP-C during cell-cycle
506 progression. *Molecular biology of the cell* 26(21):3768-3776.
- 507 36. Klare K, Weir JR, Basilico F, Zimniak T, Massimiliano L, *et al.* (2015) CENP-
508 C is a blueprint for constitutive centromere-associated network assembly
509 within human kinetochores. *The Journal of cell biology* 210(1):11-22.
- 510 37. Samejima I, Spanos C, Alves Fde L, Hori T, Perpelescu M, *et al.* (2015)
511 Whole-proteome genetic analysis of dependencies in assembly of a
512 vertebrate kinetochore. *The Journal of cell biology* 211(6):1141-1156.
- 513 38. Regnier V, Vagnarelli P, Fukagawa T, Zerjal T, Burns E, *et al.* (2005) CENP-
514 A is required for accurate chromosome segregation and sustained
515 kinetochore association of BubR1. *Molecular and cellular biology*
516 25(10):3967-3981.
- 517 39. Singh TR, Saro D, Ali AM, Zheng XF, Du CH, *et al.* (2010) MHF1-MHF2, a
518 histone-fold-containing protein complex, participates in the Fanconi
519 anemia pathway via FANCM. *Molecular cell* 37(6):879-886.
- 520 40. Yan Z, Delannoy M, Ling C, Dae D, Osman F, *et al.* (2010) A histone-fold
521 complex and FANCM form a conserved DNA-remodeling complex to
522 maintain genome stability. *Molecular cell* 37(6):865-878.
- 523 41. McKinley KL, Sekulic N, Guo LY, Tsinman T, Black BE, *et al.* (2015) The
524 CENP-L-N Complex Forms a Critical Node in an Integrated Meshwork of
525 Interactions at the Centromere-Kinetochore Interface. *Molecular cell*
526 60(6):886-898.
- 527 42. Przewlaka MR, Venkei Z, Bolanos-Garcia VM, Debski J, Dadlez M, *et al.*
528 (2011) CENP-C is a structural platform for kinetochore assembly. *Curr*
529 *Biol* 21(5):399-405.
- 530 43. Nishino T, Rago F, Hori T, Tomii K, Cheeseman IM, *et al.* (2013) CENP-T
531 provides a structural platform for outer kinetochore assembly. *The EMBO*
532 *journal* 32(3):424-436.
- 533 44. Wynne DJ & Funabiki H (2015) Kinetochore function is controlled by a
534 phospho-dependent coexpansion of inner and outer components. *The*
535 *Journal of cell biology* 210(6):899-916.

- 536 45. Anderson M, Haase J, Yeh E, & Bloom K (2009) Function and assembly of
537 DNA looping, clustering, and microtubule attachment complexes within a
538 eukaryotic kinetochore. *Molecular biology of the cell* 20(19):4131-4139.
- 539 46. Ribeiro SA, Vagnarelli P, & Earnshaw WC (2014) DNA content of a
540 functioning chicken kinetochore. *Chromosome Res* 22(1):7-13.
- 541 47. Shang WH, Hori T, Martins NM, Toyoda A, Misu S, *et al.* (2013)
542 Chromosome engineering allows the efficient isolation of vertebrate
543 neocentromeres. *Dev Cell* 24(6):635-648.
- 544 48. Magidson V, Paul R, Yang N, Ault JG, O'Connell CB, *et al.* (2015) Adaptive
545 changes in the kinetochore architecture facilitate proper spindle
546 assembly. *Nature cell biology* 17(9):1134-1144.
- 547 49. Hudson DF, Vagnarelli P, Gassmann R, & Earnshaw WC (2003) Condensin
548 is required for nonhistone protein assembly and structural integrity of
549 vertebrate mitotic chromosomes. *Dev Cell* 5(2):323-336.
- 550 50. Ribeiro SA, Gatlin JC, Dong Y, Joglekar A, Cameron L, *et al.* (2009)
551 Condensin regulates the stiffness of vertebrate centromeres. *Molecular*
552 *biology of the cell* 20(9):2371-2380.
- 553 51. Booth DG, Takagi M, Sanchez-Pulido L, Petfalski E, Vargiu G, *et al.* (2014)
554 Ki-67 is a PP1-interacting protein that organises the mitotic chromosome
555 periphery. *eLife* 3:e01641.
- 556 52. Allan J, Staynov DZ, & Gould H (1980) Reversible dissociation of linker
557 histone from chromatin with preservation of internucleosomal repeat.
558 *Proceedings of the National Academy of Sciences of the United States of*
559 *America* 77(2):885-889.
- 560 53. Allan J, Harborne N, Rau DC, & Gould H (1982) Participation of core
561 histone "tails" in the stabilization of the chromatin solenoid. *The Journal*
562 *of cell biology* 93(2):285-297.
- 563
564
565

566 **FIGURE LEGENDS**

567

568 **Figure 1: Unfolding of centromere chromatin in interphase versus**
569 **mitotic samples. A.** Schematic explaining the method employed to
570 unfold chromatin using TEEN buffer. TEEN has a low salt concentration
571 and contains EDTA as a divalent cation chelator. The excess of negative
572 charges on the DNA and the hypotonic environment together cause cells
573 to burst and the chromatin to unfold. **B.** Representative fluorescence
574 micrographs of unfolded centrochromatin fibres, detected using
575 GFP:CENP-A and DAPI. Bar, 1 μm . **C.** CLEM analysis of unfolded
576 chromatin from asynchronous cells. DAPI and GFP:CENPA were used to
577 identify typical unfolded fibres. The same regions were revisited using
578 TEM. Bar, 50 nm. Fibres visualized by TEM were analysed using multiple
579 line-scans (see representative line-scan in black (bar, 50 nm)) and pixel
580 density measurements. The data was plotted in a line graph where the
581 line profile represents an average of 5 line-scans with standard
582 deviation. Vertical red lines mark the edges of electron dense regions
583 (i.e. the width of the chromatin fibre). **D.** Box and whisker plots showing
584 the median fibre length for interphase and mitotic samples; the height
585 of the box defines the interquartile range, whiskers indicate the 10th and
586 90th percentile. Asterisks indicate statistical significance of differences in
587 fibre length between interphase and mitosis ($P < 0.0001$; Mann-Whitney
588 U test) where $n=655^{\text{fibres}}$ in total per each sample, over 3 independent
589 experiments. **E.** Bar chart showing GFP:CENP-A total fluorescence
590 plotted as a function of centromere length ($n=50$). A range of fibre
591 lengths up to 2.5 μm were tested. Data are presented as mean \pm SEM,
592 with bins of 0.5 μm increments.

593

594 **Figure 2: The centromere is composed of multiple dynamic chromatin**
595 **layers.** Multi-peak analysis using data sets of unfolded centromere
596 chromatin fibres from interphase and mitotic samples. **A** and **B** show
597 probability density histograms (white bars). X and Y axes show
598 centromere fibre length (μm) and frequency, respectively. Data are
599 allotted into 100 bins, each with a resolution of 100 nm per bin. Multi-
600 peak fitting algorithm identified putative populations of fibre lengths
601 within the data sets, depicted by discrete peaks (red lines). Best fitting
602 curve is also shown (blue line) for both samples.

603

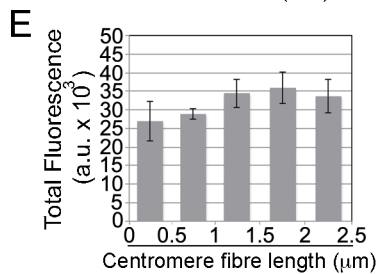
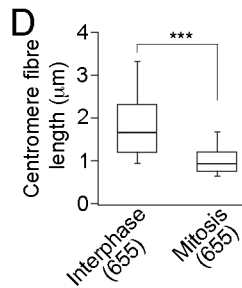
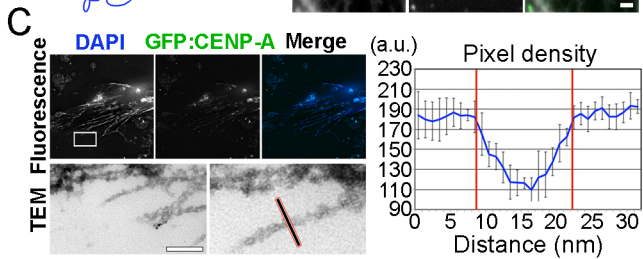
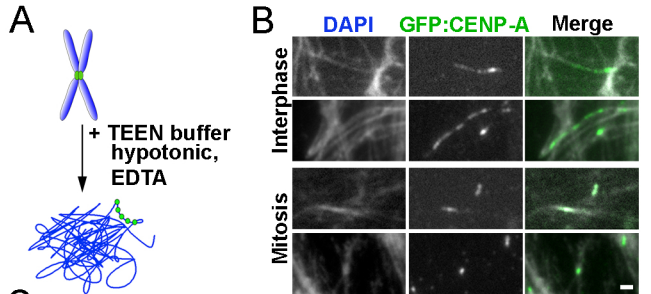
604 **Figure 3: Quantification of the steps of unfolding.** Schematic displaying
605 the sub-populations of the peaks (\blacktriangle , μm) and the distance of the
606 interval between two consecutive peaks (μm). Data obtained from
607 multi-peak fitting analysis in Fig. S7.

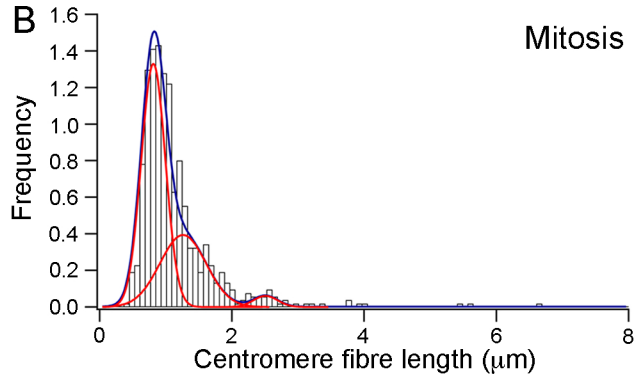
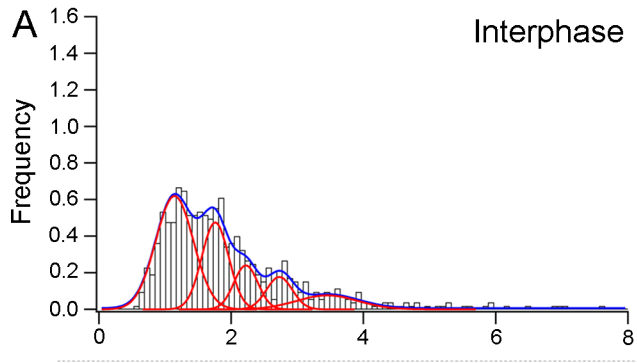
608

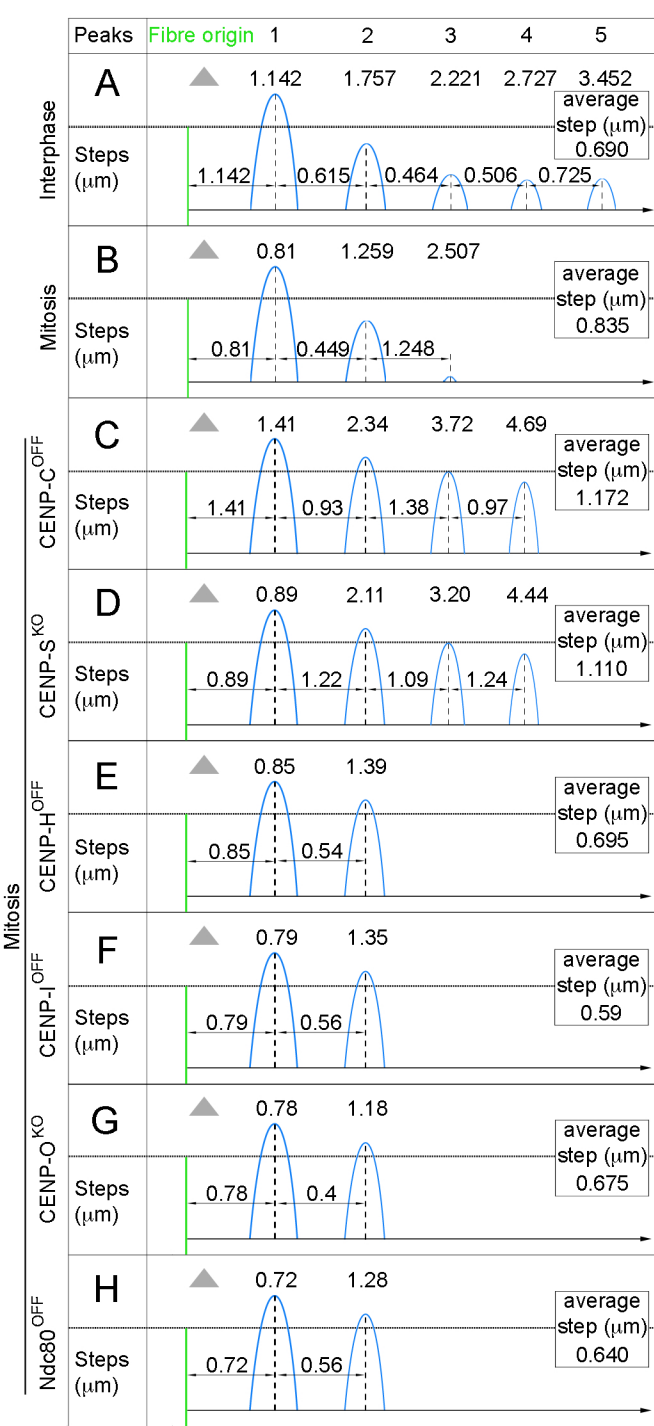
609 **Figure 4: Comparison of models for centrochromatin structure. A.**
610 Solenoid in which CENP-A (red) and H3 (grey) nucleosomes are
611 organized at centromeres into helical gyres (1 gyre per “subunit”) or **B.**
612 Loops clustered next to each other (1 loop per “subunit”). These two
613 models were first proposed by (3). Gyres and loops diagrammed here
614 could both generate unfolded fibres in presence of TEEN with an
615 unfolded length of roughly $0.5 \mu\text{m}$. **C.** Boustrophedon model consisting
616 of a stack of planar sinusoidal patches (layers) of centrochromatin (1
617 layer is a subunit). As a response to TEEN buffer, single layers of the
618 boustrophedon might unfold into chromatin fibres $0.5 \mu\text{m}$ long.

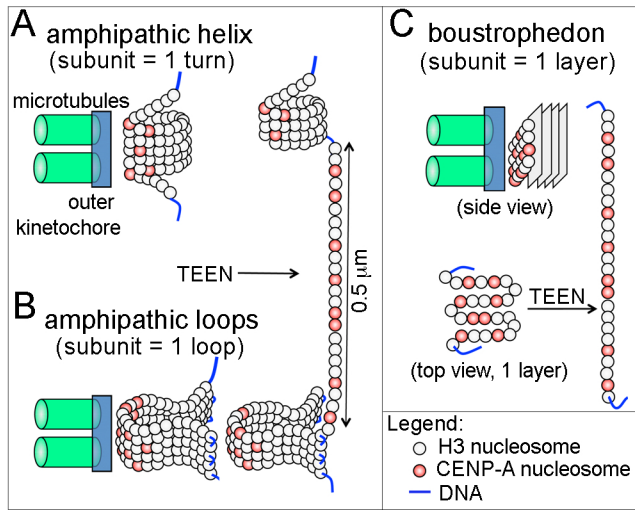
619

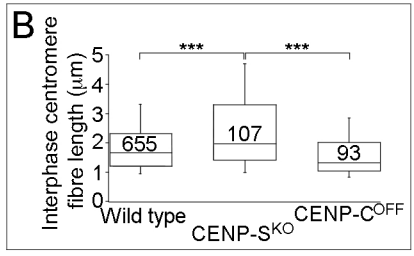
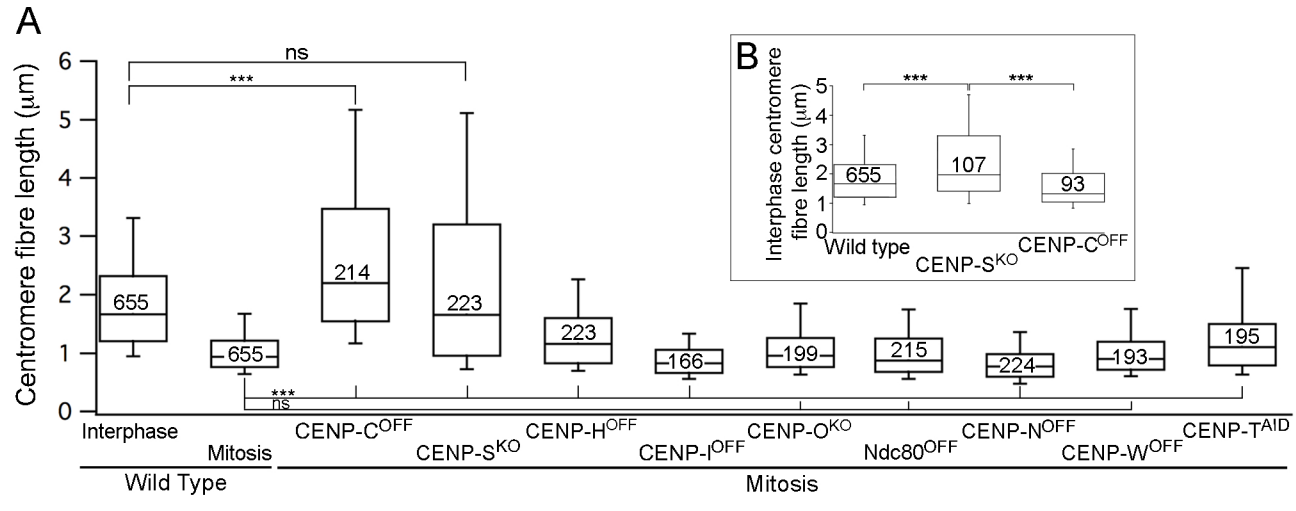
620 **Figure 5: Unfolding of centromere chromatin in CENP mutants. A and B**
621 Box and whisker plots displaying the spread of the data sets of unfolded
622 fibre length measured in: **A.** wild type and the indicated mutants, after
623 being blocked in nocodazole; **B.** wild type and indicated mutants
624 asynchronous cells. The height of the box defines the interquartile
625 range, whiskers indicate the 10th and 90th percentile. The n number is
626 specified in each box. **A.** Each conditional knockout cell line has been
627 tested for significant difference against unfolded fibres from control
628 interphase or control mitosis. Only statistically insignificant comparisons
629 are shown in the graph (Mann-Whitney U test). **B.** Mann-Whitney U test
630 was performed confirming statistically significant differences between
631 the mutants and wild type fibres.
632











SUPPLEMENTARY MATERIALS AND METHODS

Cell culture

Chicken B lymphoma DT40 cells were grown in RPMI 1640 medium supplemented with 10% FBS, 1% chicken serum and 1% penicillin/streptomycin at 39°C in 5% CO₂. CENP-C (30), CENP-H (27), CENP-I (28) and Ndc80 (29), CENP-T^{AID} (32) conditional knockout cell lines were transfected with GFP:GgCENP-A cloned in pEGFPC1 vector with 17-amino acid linker (50). Cell lines stably expressing GFP:GgCENP-A were obtained by co-electroporation with puromycin, hygromycin and geneticin-resistant markers. CENP-N and CENP-W conditional knockout cell lines stably expressing GFP:CENP-A were previously generated (4). The addition to the media of 500 ng/ml of doxycycline or auxin at the final concentration of 125 μM destroyed the expression of the rescuing cDNA. DT40 cells were blocked in mitosis by treating with 500 ng/ml nocodazole for 12 hours.

Cell vital counts using Trypan Blue

For cell counts experiments, 1 part of trypan blue was added to 1 part of cell suspension at room temperature. DT40 cells were maintained at a concentration of 20×10^4 cells/ml at each dilution time.

CENP-A total fluorescence quantification

For 50 fibres randomly picked images were deconvolved and projected into ImageJ (National Institute of Health, Bethesda, MD) and the area occupied by CENP-A signal along each fibre was highlighted by thresholding and then selected with the magic wand. The fluorescence,

measured in ImageJ, was annotated. Graphs were produced in Microsoft Excel.

Correlative light electron microscopy (CLEM) of unfolded fibres

The CLEM protocol was adapted from a previously established method (51). DT40 cells expressing GFP:CENPA were seeded onto ConA coated glass-bottomed gridded dishes (MatTeK Corporation, USA), and left to adhere for 1 hour. Fibres were prepared using the standard protocol until the point of fixation. Fibres were fixed for 1 hour with 3% glutaraldehyde and 0.5% formaldehyde in 0.2 M sodium cacodylate buffer containing 5 µg/mL Hoechst. Fibres were washed with PBS and imaged in PBS using a DeltaVision microscope (Applied Precision) where GFP:CENP-A centrochromatin was detected. Transmitted light was used to map cell positions via reference coordinates. The reference images allowed for the correlative re-identification of cells of interest by electron microscopy. DeltaVision acquisition was followed by treatment with tannic acid (0.1% in water) for 20 minutes, followed by osmication (1% osmium tetroxide in PBS) for 1 hour. Samples were then washed with PBS, ddH₂O and 30% ethanol before the incubation in uranyl acetate (0.5% in 30% ethanol) for 1 hour. Next, fibres were dehydrated using a graded series of ethanol washes. Following dehydration, samples were infiltrated with ethanol:resin mixtures (2:1 and 1:1) for 20 minutes each. Finally, cells were embedded in 100% resin (TAAB), with a gelatin capsule of resin covering the cells of interest, before curing at 60 °C for 3 days. Polymerised resin blocks were sectioned and post stained as routine. Samples were viewed using a Phillips CM120 BioTwin

transmission electron microscope (FEI) and micrographs acquired using a Gatan Orius CCD camera (Gatan).

Electron microscopy of mitotic nucleosomes

Chromosomes isolated from colcemid arrested HeLa cells were centrifuged at 1,400 g for 20 minutes at 4°C onto carbon-coated grids and rinsed in 0.4% Photoflo (Kodak). Grids were fixed in TEEN buffer containing 1% glutaraldehyde for 1-2 hours at 4°C. Grids were consecutively dipped into 1% phosphotungstic acid in 71% ethanol (15 sec), 95% ethanol (15 sec), 0.4% Photoflo (5 sec), blotted dry and rotary shadowed using platinum:paladium. Images were obtained with a Philips EM-300 at 80 kV (23).

Electron microscopy of interphase nucleosomes

Size-fractionated chromatin fibres were isolated from chicken erythrocytes and prepared for electron microscopy as previously described (52, 53). Benzylalkyldimethylammonium chloride (BAC) (Sigma) was added to the chromatin to a concentration of 2×10^{-4} % (v/v). The mixture was incubated at RT for 30 mins. The chromatin was spread on formvar/carbon coated copper grids (TAAB). The grids were washed with ddH₂O and 90% ethanol and allowed to dry. For contrast enhancement the grids were rotary-shadowed by a Leica ACE600 at a pressure of $1-2.5 \times 10^{-5}$ mbar. Rotating samples were coated with 2 nm platinum (measured by a quartz sensor) at an elevation angle of 7°. The grids were examined by a JEOL JEM-1400 Plus TEM, operated at a magnification of 20K, 80kV. Electron micrographs were acquired using GATAN OneView camera.

Indirect immunofluorescence

To analyse GFP:CENP-A localization an immuno-stain for CENP-T was performed. Cells were seeded onto Concanavaline A (ConA) coated coverslips and left to adhere for 1 hour in the incubator prior to fixation. Cells were washed with warm PBS and fixed with pre-warmed 4% formaldehyde/PBS solution for 10 minutes. Cells were permeabilised by incubating coverslips for 2 minutes in 0.15% Triton X-100/PBS solution. Cells were blocked in 1% BSA/PBS solution for 1 hour at room temperature and subsequently incubated with primary rabbit anti-GgCENP-T antibody diluted 1:1000 (14) in the blocking solution for 1 hour. Prior to secondary antibody incubation cells were washed three times in 0.1% Tween20/PBS solution. Fluorophore conjugated secondary antibody (Alexa Fluor 594; Jackson ImmunoResearch Laboratories, Inc.) was diluted 1:1000 in the blocking solution and the incubation 45 minutes long. Several washes followed and coverslips were finally mounted on slides using Vectashield containing DAPI (Vector Labs) as antifade media. 3D intact cell image stacks were deconvolved, quick projected and saved as tiff images.

SDS-PAGE and immunoblotting

Cell lysates were sonicated and boiled in sample buffer (5% sucrose, 1% SDS, 16.67 mM Tris-HCl pH 6.8, 0.67 mM EDTA, 10% β -Mercaptoethanol (v/v), 0.01% bromophenol blue). Lysates were resolved in SDS-PAGE with 12% polyacrylamide gels (BioRad electrophoresis apparatus). After transferring the proteins to a nitrocellulose membrane (Amersham, GE) blocking with 3% low fat milk in 0.05% Tween20/PBS solution for 1 hour

was performed prior immunoblotting. Primary antibodies used for immunoblotting included: mouse anti- α tubulin (1:5000, B512 Sigma), rabbit anti-GgCENP-A (1:1000) and rabbit anti-GFP (1:1000, Life Technologies). Membranes were washed in 0.05% Tween20/PBS solution and incubated with secondary antibodies (IRDye 800 or IRDye 680; Li-Cor Biosciences) and abundantly washed before proceeding to the detection using a CCD scanner (Odyssey; Li-Cor Biosciences). Quantification of CENP-A bands was performed using ImageJ and normalized for the tubulin signal.

SUPPLEMENTARY FIGURE LEGENDS:

Supplementary Figure 1. Characterization of DT40 cells stably expressing GFP:CENP-A. **A.** Western analysis of whole cell lysate prepared from DT40 cells stably expressing GFP:CENP-A or the wild type cell line (control). The membrane was probed with primary antibodies recognising CENP-A, tubulin and GFP. A LI-COR system was used for imaging. **B.** Indirect immunofluorescence of cells expressing GFP:CENP-A. Cells were probed with anti CENP-T antibody (red). Mitotic stages are indicated on the left of the panels. Scale bar, 5 μ m. **C.** Representative image of DT40 cells stably expressing GFP:CENP-A where CENP-A signal co-localizes with CENP-T on unfolded fibres. Scale bar, 5 μ m.

Supplementary Figure 2. Increasing the number of bins increases the resolution of the histograms. **A.** Two columns of frequency histograms containing fibre length data for interphase and mitotic samples. Columns show progressive improvements in the histogram resolution by adjusting the number of bins and bin width (bin width indicated in

brackets); 50 bins (200 nm), 60 bins (166 nm), 80 bins (125 nm) and 100 bins (100 nm). The scale on the y axis has been kept different for interphase and mitosis to allow a better visualization of the peaks in the two data sets. **B.** Frequency histograms containing both data sets allotted into 100 bins (100 nm) are merged together in one plot with the same scale on the y axis.

Supplementary Figure 3. Quantification of the inter-nucleosome distance in interphase. A. TEM of mitotic chromosomes centrifuged onto a carbon film after TEEN buffer treatment. The center-to-center distance between adjacent nucleosomes (n=203) was determined to be 20.4 ± 0.68 nm (mean \pm SEM). The inset represent a 2 X zoom. Scale bar, 50 nm. **B.** Micrograph of interphase chromatin from chicken erythrocytes spread onto grids and imaged by TEM following rotary shadowing. The center-to-center distance between adjacent nucleosomes (n= 65) was determined to be 38.71 ± 1.6 nm (mean \pm SEM). The inset represent a 2 X zoom. Scale bar, 50 nm. **C.** Schematic of the calculations used to predict the DNA content at the chicken centromere.

Supplementary Figure 4. Characterization of DT40 conditional knockouts or deletion cell lines stably expressing GFP:CENP-A. A. Indirect immunofluorescence of cells expressing GFP:CENP-A probed with anti CENP-T antibody (red). The localization of GFP:CENP-A is at the kinetochore in all the conditions analysed. Scale bar, 5 μ m. **B.** Growth curves of mutant cell lines plus or minus doxycycline and DT40 control

cell line. **C.** Western blot of whole cell lysate of samples prior to the addition of doxycycline.

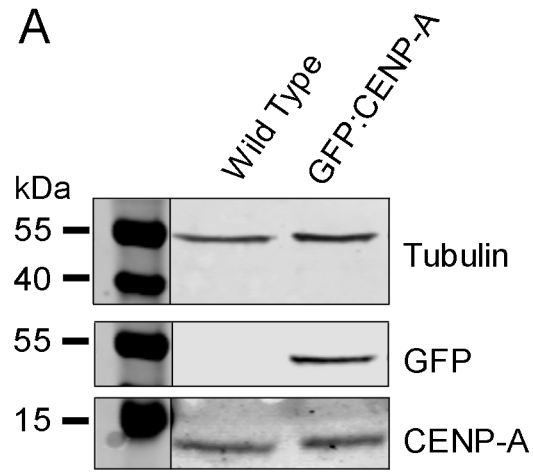
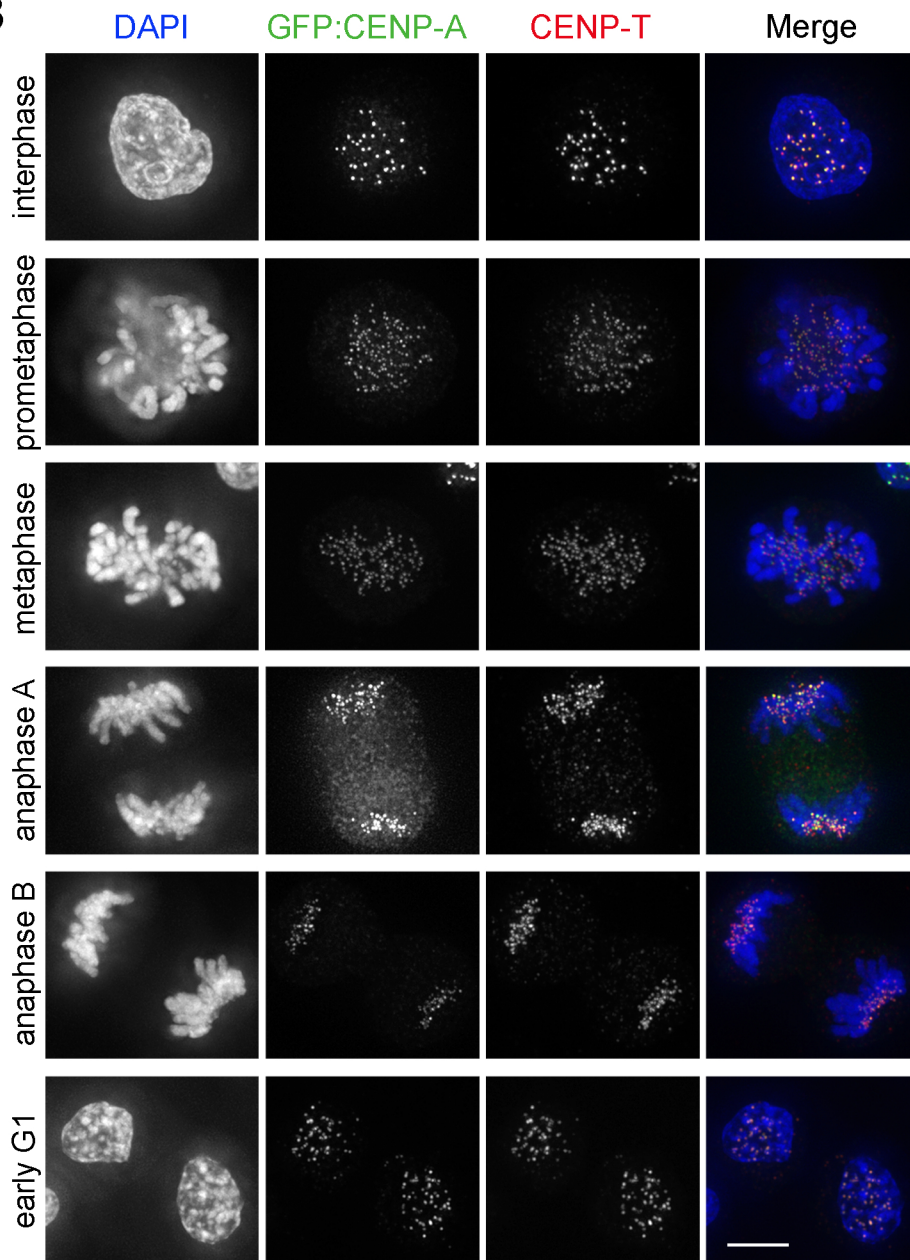
Supplementary Figure 5. Characterization of CENP-N and CENP-W conditional knockouts or inducible auxin-degron for CENP-T cell lines stably expressing GFP:CENP-A. **A.** Indirect immunofluorescence of cells expressing GFP:CENP-A and probed with anti CENP-T antibody (red). The localization of GFP:CENP-A is at the kinetochore in all the conditions analysed. Scale bar, 5 μ m. **B.** Growth curves of mutant cell lines in the presence of doxycycline. The growth curves for AID-CENP-T:CENP-T^{ON/OFF} cells plus and minus auxin are shown in (32), Figure 2C. These cells begin to die within 24 hours of the addition of auxin. **C.** Western blot of whole cell lysate of samples with no addition of doxycycline or auxin.

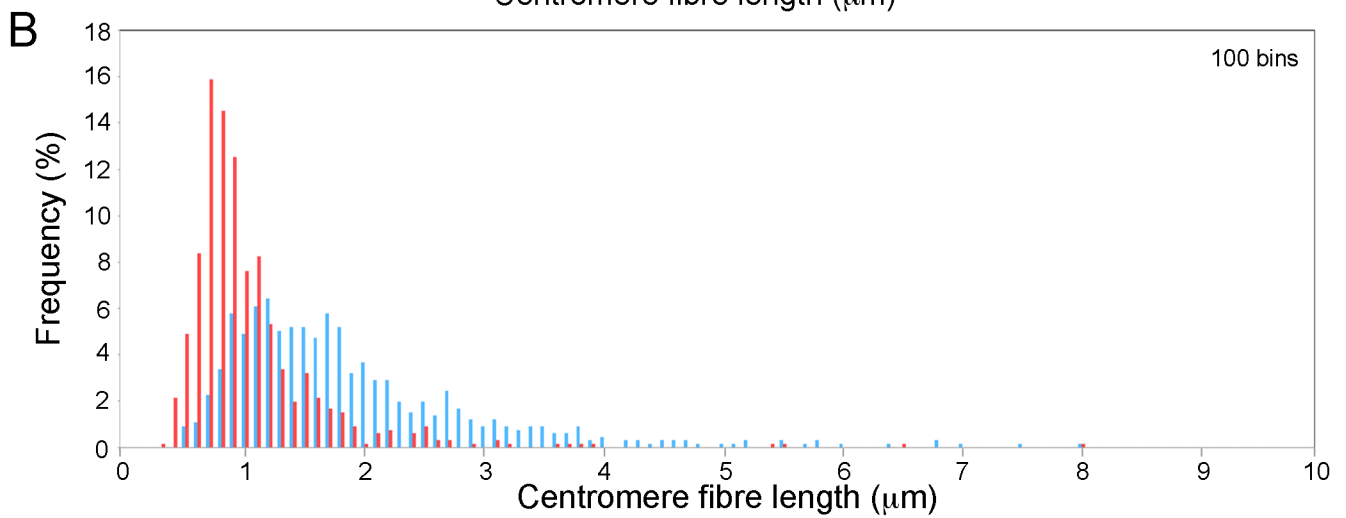
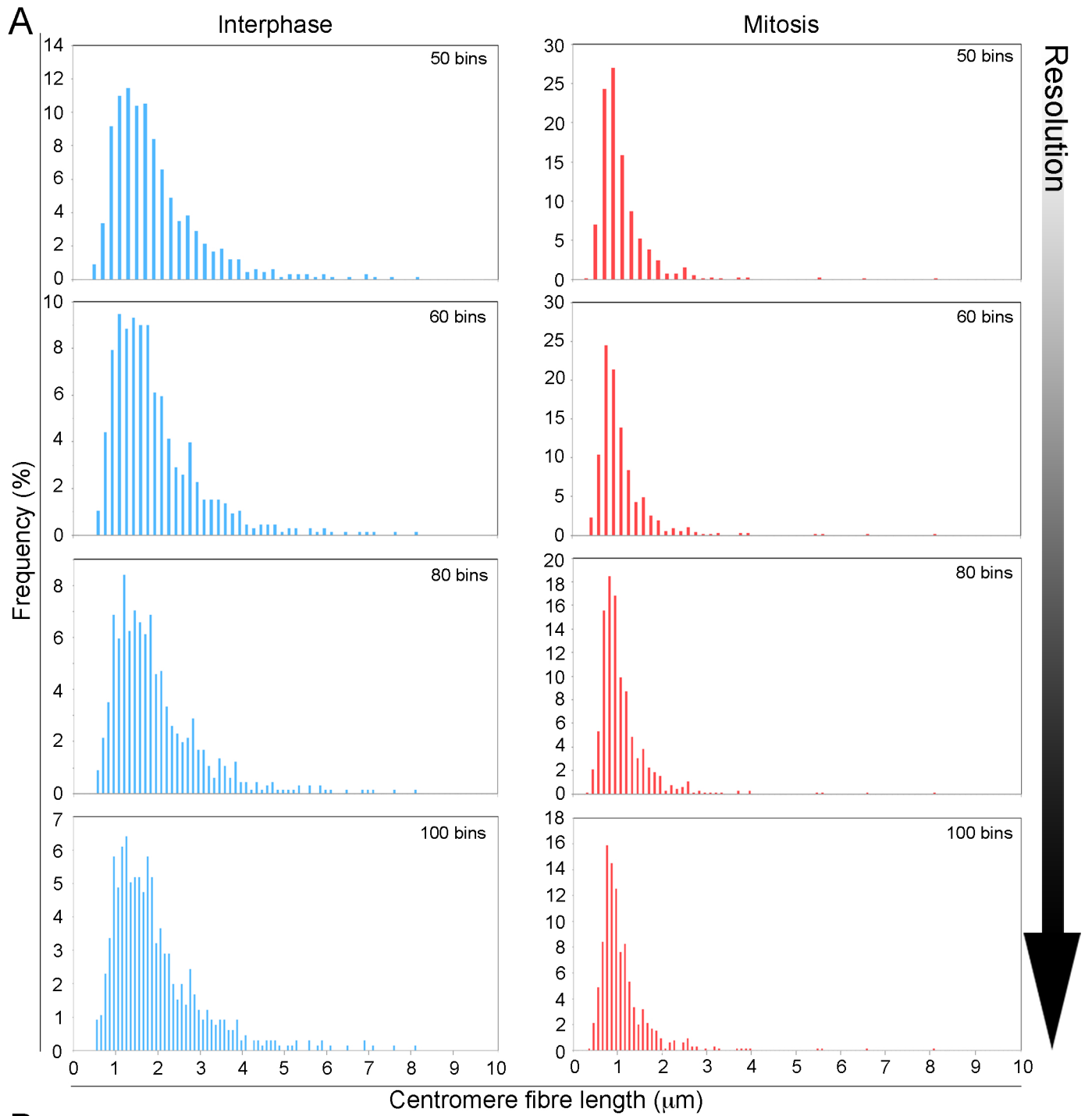
Supplementary Figure 6. Quantification of CENP-A levels. The quantification of the bands for endogenous CENP-A, GFP:CENP-A and tubulin from the blots shown in Figs. S4C (**A**) or Fig. S5C (**B**) was performed using ImageJ. The graphs show the levels of endogenous CENP-A (blue) and GFP:CENP-A (red) after normalization with tubulin.

Supplementary Figure 7. Multi-peak analysis of centromere chromatin fibres unfolding data sets in CENP mutant cell lines. For all the panels: the bottom part of each graph show probability density histograms, where x and y axes show frequency and centromere fibre length (μ m) respectively; the data sets are divided in 100 bins (interphase and mitosis wild type – Figs. 2, S2) with a resolution of 100 nm or 50 bins (mutants) with a resolution of 200 nm per bin. Histograms of

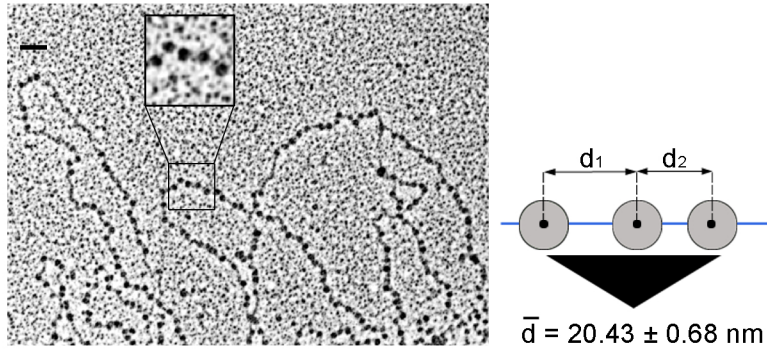
centromere fibre length showing putative populations of fibre lengths within the data sets underlined by the diverse peaks (red lines). The scale on the y axis has been kept different for the different mutants to allow a better visualization of the peaks in the data sets. The best fitting curve is shown (blue line) for all the samples. Inset, fluorescent images of centromere fibres are shown for each mutant; DAPI, GFP and merge respectively. Scale bar, 1 μm . The upper part of each graph highlights the amount of residuals.

Supplementary Figure 8. Centromerichromatin unfolding analysis CENP-N, CENP-W and CENP-T depleted cells. A. Schematic displaying the sub-populations of the peaks (μm) and the distance of the interval between two consecutive peaks (μm). Data obtained from multi-peak fitting analysis in panel B. **B.** For all panels: the bottom part of each graph show probability density histograms, where x and y axes show frequency and centromere fibre length (μm) respectively; the data sets are divided in 50 bins with a resolution of 200 nm per bin. Histograms of centromere fibre length showing putative populations of fibre lengths within the data sets underlined by the diverse peaks (red lines). The scale on the y axis has been kept different for the different mutants to allow a better visualization of the peaks in the data sets. The best fitting curve is shown (blue line) for all the samples. Inset, fluorescent images of centromere fibres are shown for each mutant; DAPI, GFP and merge respectively. Scale bar, 1 μm . The upper part of each graph highlights the amount of residuals.

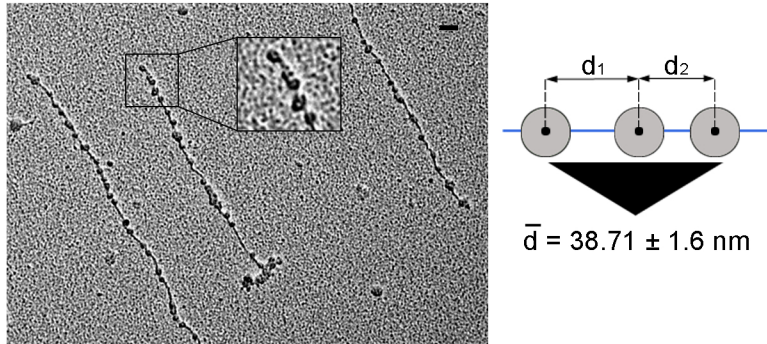
A**B****C**



A



B



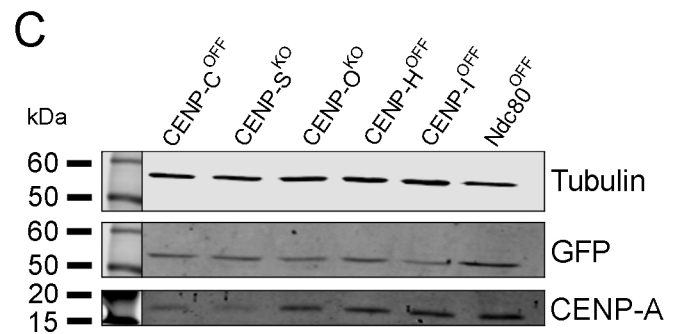
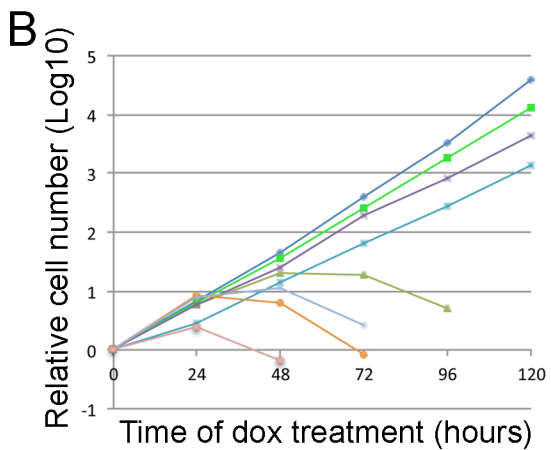
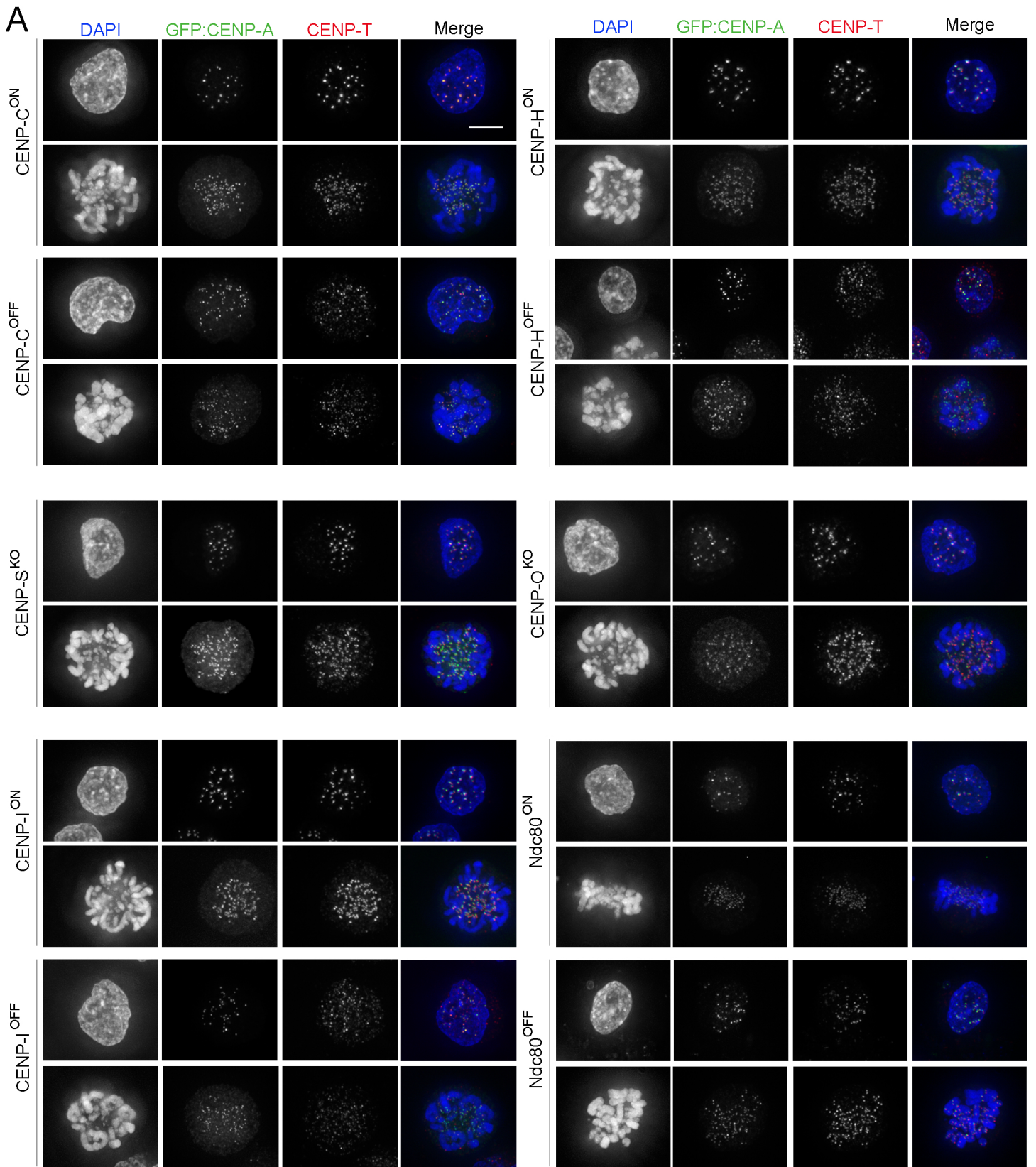
C

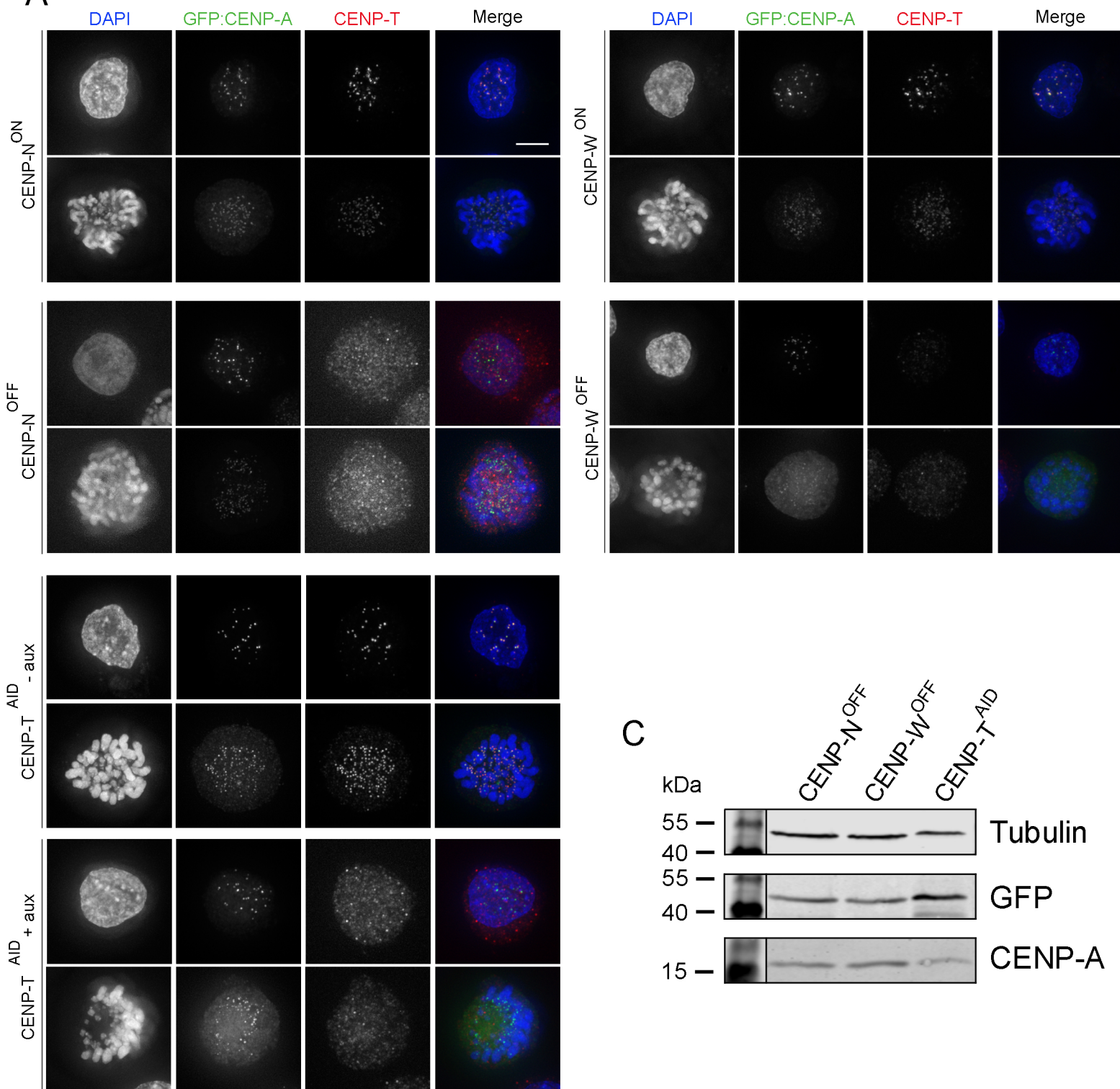
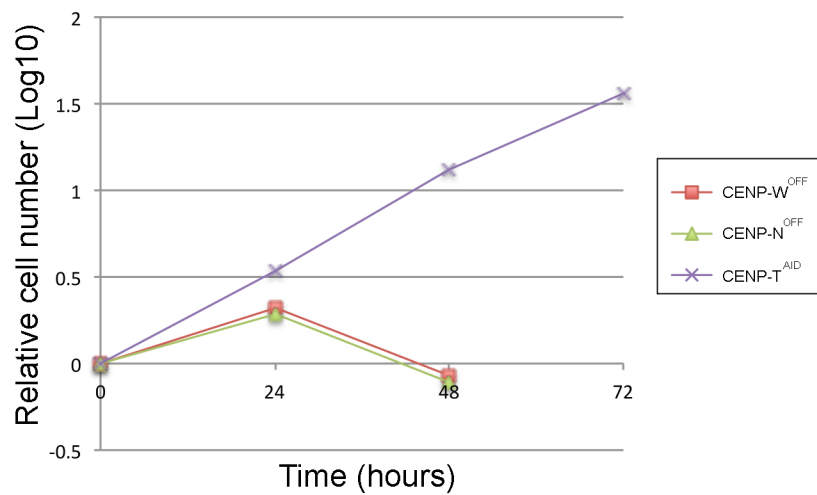
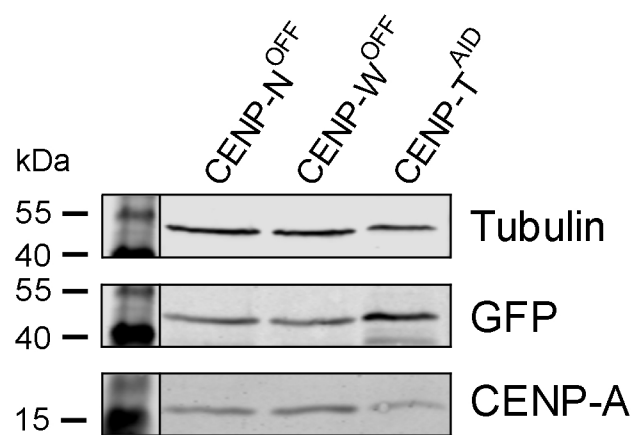


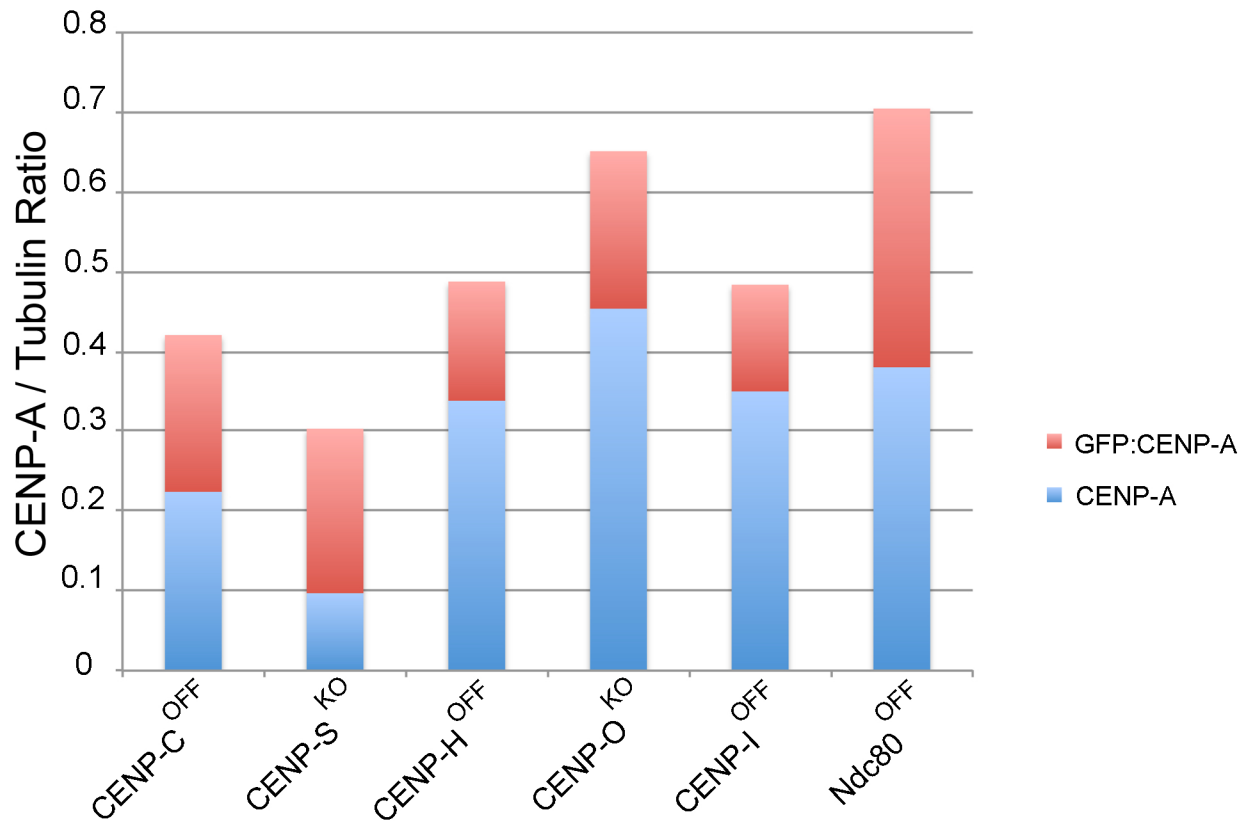
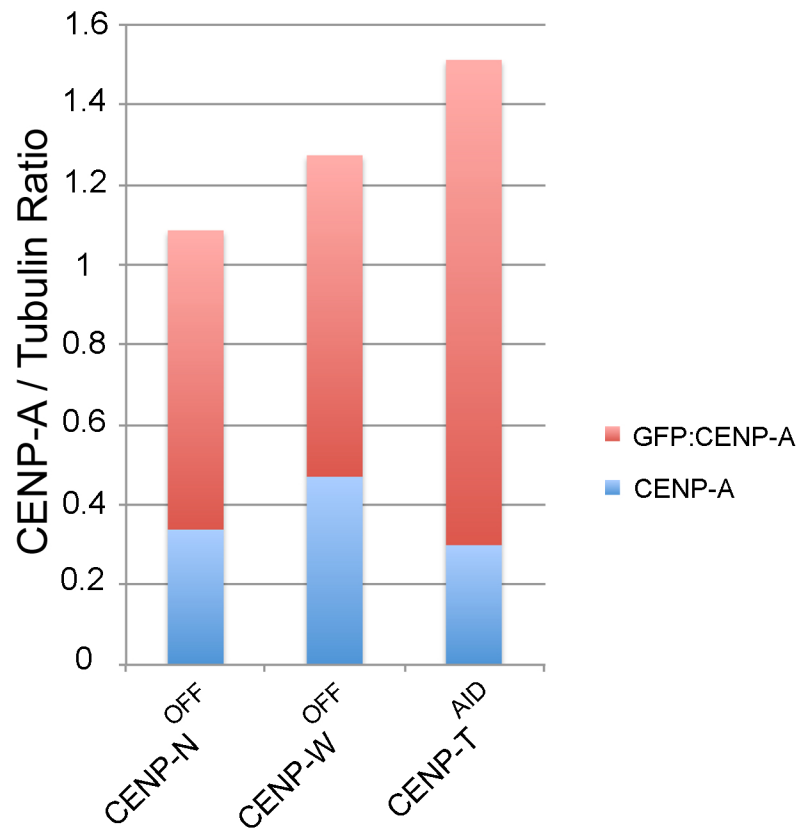
INTERPHASE:	690 nm	\div	38.71 nm	$=$	17.8 nucleosomes	\times	5 layers	$=$	89 nucleosomes
	Mean step of unfolding		internucleosome distance		per layer		sub-populations of unfolded fibers		total in the DT40 centromere
MITOSIS:	835 nm	\div	20.43 nm	$=$	40.8 nucleosomes	\times	3 layers	$=$	122.4 nucleosomes

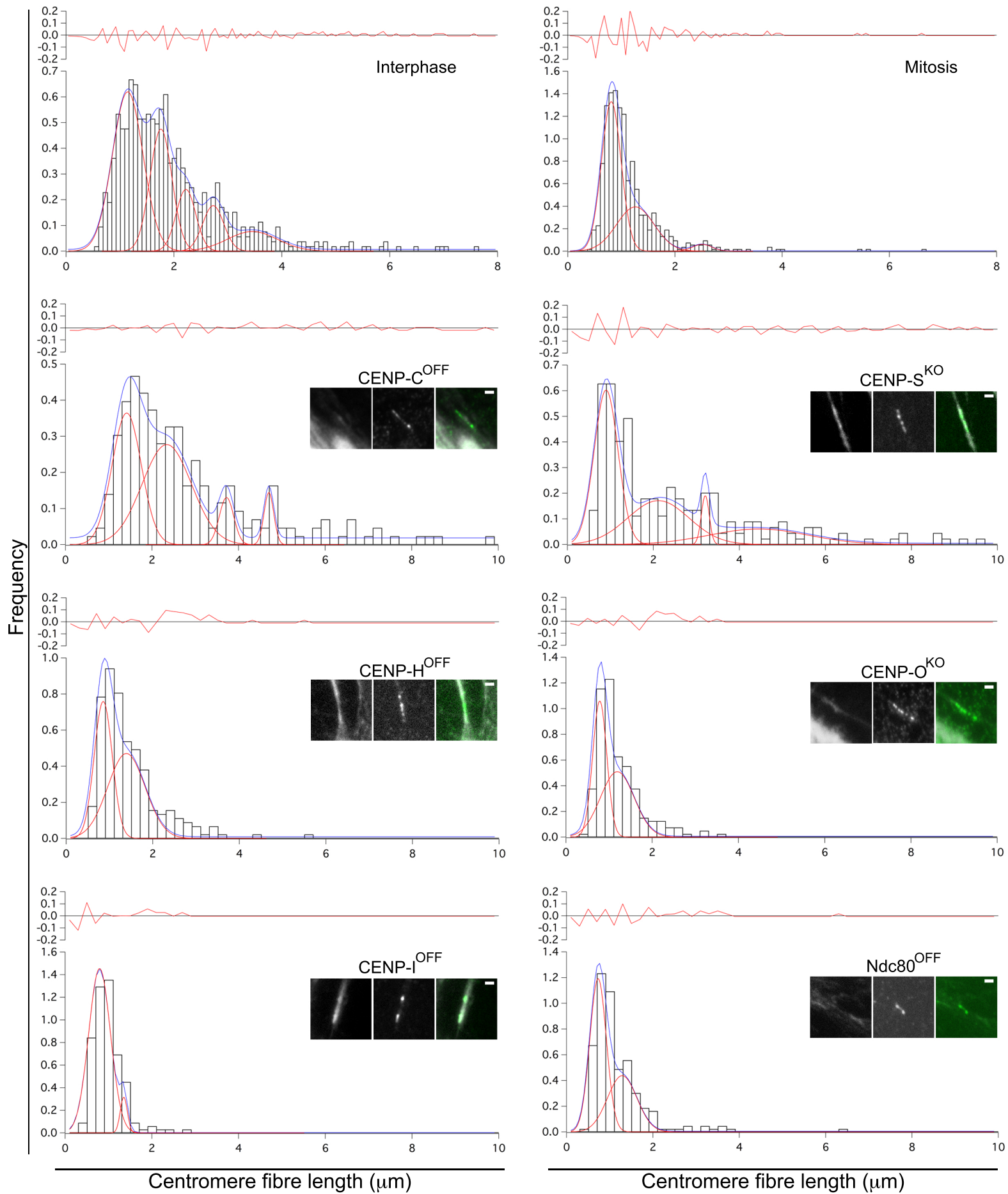
$89 \text{ nucleosomes} \times 200 \text{ bp} = 17.8 \text{ Kbp DNA in centromere}$
 $122.4 \text{ nucleosomes} \times 200 \text{ bp} = 24.4 \text{ Kbp DNA in centromere}$

total in the DT40 centromere ~ DNA + linker on a nucleosome

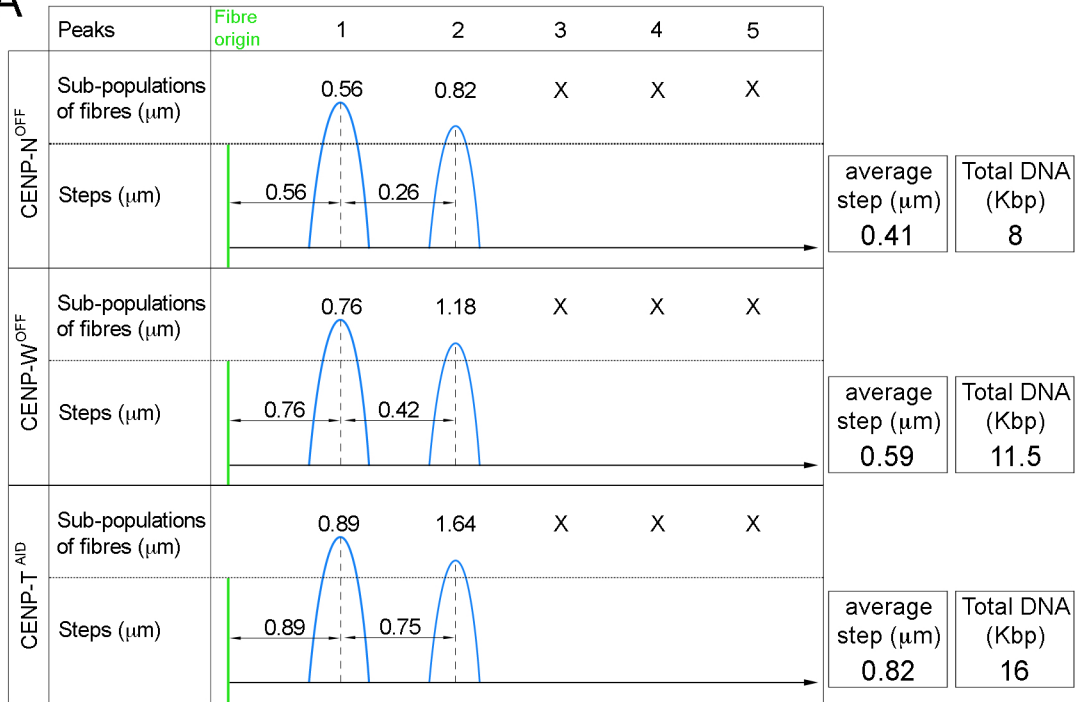


A**B****C**

A**B**



A



B

